Hydrolytic activity of human Nudt16 enzyme on dinucleotide cap analogs and short capped oligonucleotides

RENATA GRZELA,[1] KAROLINA NASILOWSKA,[2] MACIEJ LUKASZEWICZ,[2] MICHAL TYRAS,[1] JANUSZ STEPINSKI,[1] MARZENA JANKOWSKA-ANYSZKA,[3] ELZBIETA BOJARSKA,[1] and EDWARD DARZYNKIEWICZ[1,2]

[1]Centre of New Technologies, University of Warsaw, 02-097 Warsaw, Poland
[2]Division of Biophysics, Institute of Experimental Physics, Faculty of Physics, University of Warsaw, 02-097 Warsaw, Poland
[3]Faculty of Chemistry, University of Warsaw, 02-091 Warsaw, Poland

ABSTRACT

Human Nudt16 (hNudt16) is a member of the Nudix family of hydrolases, comprising enzymes catabolizing various substrates including canonical (d)NTPs, oxidized (d)NTPs, nonnucleoside polyphosphates, and capped mRNAs. Decapping activity of the *Xenopus laevis* (X29) Nudt16 homolog was observed in the nucleolus, with a high specificity toward U8 snoRNA. Subsequent studies have reported cytoplasmic localization of mammalian Nudt16 with cap hydrolysis activity initiating RNA turnover, similar to Dcp2. The present study focuses on hNudt16 and its hydrolytic activity toward dinucleotide cap analogs and short capped oligonucleotides. We performed a screening assay for potential dinucleotide and oligonucleotide substrates for hNudt16. Our data indicate that dinucleotide cap analogs and capped oligonucleotides containing guanine base in the first transcribed nucleotide are more susceptible to enzymatic digestion by hNudt16 than their counterparts containing adenine. Furthermore, unmethylated dinucleotides (GpppG and ApppG) and respective oligonucleotides (GpppG-16nt and GpppA-16nt) were hydrolyzed by hNudt16 with greater efficiency than were m^7GpppG and m^7GpppG-16nt. In conclusion, we found that hNudt16 hydrolysis of dinucleotide cap analogs and short capped oligonucleotides displayed a broader spectrum specificity than is currently known.

Keywords: decapping enzymes; nudix hydrolases; cap analogs; cap hydrolysis; capped oligonucleotides

INTRODUCTION

Eukaryotic mRNAs are modified with a covalently attached 7-methylguanosine cap at the 5′ end, with an unusual 5′–5′ pyrophosphate bond (Furuichi and Shatkin 2000; Ghosh and Lima 2010). Cap hydrolysis is a critical step in mRNA turnover. mRNA decay can occur via two general pathways, in the 3′–5′ or 5′–3′ direction, both initiated by shortening of the poly(A) tail (Meyer et al. 2004). Therefore, different classes of decapping enzymes have been reported to function in these processes (Grudzien-Nogalska and Kiledjian 2017; Valkov et al. 2017). The 3′ end mRNA decay is carried out by a cytoplasmic multisubunit exosome complex (Schaeffer et al. 2009) and the resulting cap dinucleotides (or short oligonucleotides) are subsequently hydrolyzed by the scavenger decapping enzyme DcpS (Liu et al. 2002), which utilizes an evolutionarily conserved HIT motif to bind substrates and cleave the pyrophosphate bond within the cap, thereby releasing m^7GMP (Liu et al. 2004). Cap removal from long mRNAs in the 5′–3′ decay pathway is carried out by two specific enzymes, Dcp2 and Nudt16, both members of the Nudix hydrolase superfamily, which hydrolyze various substrates composed of a nucleoside diphosphate linked to another moiety X. Their catalytic activity depends on the highly conserved Nudix box within a sequence of 23 amino acids, $GX_5EX_7XREUXEEXGU$, where U is a hydrophobic residue (usually Ile, Leu, or Val), and X may be any residue (Bessman et al. 1996). This sequence is located in a loop–helix–loop structural motif and the Glu residues within the core of the motif, REX2EE, are essential for binding divalent metal ions, Mn^{2+} or Mg^{2+} (Bessman et al. 1996). Nudix enzymes hydrolyze substrates usually through nucleophilic substitution at phosphorus, with variations in the type and number of divalent cations (Mildvan et al. 2005; McLennan 2006).

The most well characterized and widely conserved eukaryotic decapping enzyme is Dcp2, identified in yeast (Steiger

Corresponding authors: r.grzela@cent.uw.edu.pl, e.bojarska@cent.uw.edu.pl

Article is online at http://www.rnajournal.org/cgi/doi/10.1261/rna.065698.118.

et al. 2003), nematodes (Cohen et al. 2005), plants (Iwasaki et al. 2007), and humans (Picirillo et al. 2003). Dcp2 cleaves m^7G-capped and $m_3^{2,2,7}$G-capped RNAs, thereby releasing m^7GDP/$m_3^{2,2,7}$GDP and 5′ monophosphate RNA (Picirillo et al. 2003; Steiger et al. 2003; Cohen et al. 2005; Iwasaki et al. 2007). Dcp2 recognizes mRNA by interacting with the cap structure and the RNA body (Deshmukh et al. 2008; Li et al. 2008), and preferentially utilizes RNAs longer than 25 nucleotides (nt). Its activity is tightly regulated by several proteins known to interact with Dcp2 in cytoplasmic foci called P-bodies (van Dijk et al. 2002; Franks and Lykke-Andersen 2008; Arribas-Layton et al. 2013). The presence of the second decapping enzyme Nudt16 has been reported in mammalian cells (Song et al. 2010; Lu et al. 2011). Nudt16 was initially identified in *Xenopus* as a U8 snoRNA decapping enzyme (termed as X29) (Ghosh et al. 2004; Peculis et al. 2007) and has also been proposed as a nucleolar decapping enzyme that is conserved in metazoans, but is absent in *S. cerevisiae*, *C. elegans*, and *Drosophila* (Taylor and Peculis 2008). Nudt16 orthologs were identified in 57 different organisms, both invertebrates and vertebrates (Trésaugues et al. 2015). Nudt16 distribution across metazoans implies an evolutionarily conserved biological role for this enzyme, which can cleave the m^7G cap from pre-mRNA and mature mRNA prior to export, and the $m_3^{2,2,7}$A cap from snRNA and snoRNA (Lange et al. 1998). Further studies revealed the abundance of hNudt16 in both the nucleus and cytoplasm (Song et al. 2010; Lu et al. 2011), demonstrating the pleiotropic decapping activity of this enzyme. Since its function partially overlaps with Dcp2 hydrolytic activity in mammalian cells, hNudt16 was proposed as the second decapping enzyme involved in the 5′→3′ degradation of cytoplasmic mRNAs. Although both enzymes can initiate mRNA decay by hydrolyzing the cap structure, distinct roles for Dcp2 and Nudt16 in specific mRNA degradation pathways were reported (Li et al. 2011). Nonsense-mediated mRNA decay is mostly mediated by Dcp2, while ARE-containing mRNAs and miRNA can be degraded by either Dcp2 or Nudt16.

A comparison of hNudt16 in vitro catalytic activity toward U8 snoRNA, luciferase mRNA, and influenza NP mRNA has shown similar decapping efficiency for these substrates (Lu et al. 2011). The capability to cleave the cap from the three RNAs was very effective in the presence of Mn^{2+} and Mg^{2+}, but drastically weaker with Co^{2+} and Zn^{2+}. Interestingly, Nudt16 was also characterized as a "housecleaning" enzyme specialized in eliminating hazardous (deoxy)inosine diphosphate from the nuclear nucleotide pool (Iyama et al. 2010). The hydrolytic activity of recombinant hNudt16 was assessed in vitro with different purine nucleoside diphosphates (Trésaugues et al. 2015). Recent studies also reported that hNudt16 can process protein ADP-ribosylation (Daniels et al. 2015; Palazzo et al. 2015). The latest study (Carreras-Puigvert et al. 2017) analyzed human Nudix hydrolases on the basis of the deposited PDB structures and with numerous substrates, comprising standard and modified (deoxy)nucleotides, adenine dinucleotide polyphosphates, nicotinamide adenine dinucleotides, or the standard 5′ cap. However, the cap structures, which are the subject of our study, were not investigated previously.

To further characterize the decapping activity of human Nudt16, we analyzed the substrate properties of several capped dinucleotides (m^7GpppG, m^7Gpppm$^{2'\text{-}O}$G, m^7GpppA, m^7Gpppm$^{2'\text{-}O}$A, and $m_3^{2,2,7}$GpppG) and short oligonucleotides (m^7GpppG-16nt, m^7Gpppm$^{2'\text{-}O}$G-16nt, m^7GpppA-16nt, m^7Gpppm$^{2'\text{-}O}$A-16nt, m^7GpppG-34nt, and m^7Gpppm$^{2'\text{-}O}$G-34nt). Simultaneously, we also analyzed unmethylated dinucleotides (GpppG, ApppG) and their oligonucleotide counterparts (GpppG-16nt, GpppA-16nt, and GpppG-34nt). Analysis of hNudt16 hydrolysis of dinucleotide cap analogs and short capped oligonucleotides displayed a much broader spectrum for enzyme specificity than is currently known.

RESULTS

Hydrolytic activity of hNudt16 on dinucleotides

Human Nudt16 is known to display activity toward various mononucleotides and long RNAs (Ghosh et al. 2004; Peculis et al. 2007; Taylor and Peculis 2008; Iyama et al. 2010; Song et al. 2010; Li et al. 2011; Lu et al. 2011; Trésaugues et al. 2015). In the present study, we investigated the hydrolytic activity of hNudt16 on dinucleotides and short oligonucleotides. Initially, we performed an activity screening assay to identify potential dinucleotide substrates for this hNudt16. The hydrolytic reactions of several dinucleotides (GpppG, ApppG, m^7GpppG, m^7Gpppm$^{2'\text{-}O}$G, m^7Gpppm^{7}G, m^7GpppA, m^7Gpppm$^{2'\text{-}O}$A, and $m_3^{2,2,7}$GpppG) (Fig. 1) catalyzed by hNudt16 were studied under the same experimental conditions (substrate and enzyme concentration, buffer composition, and temperature), which allowed for direct comparison of their hydrolytic susceptibilities. Reaction progress was monitored through HPLC analysis. Reduction in chromatographic peaks corresponding to the substrate was accompanied by the peaks characteristic of hydrolysis products (Fig. 2). The results of all investigated compounds are summarized in Table 1. Our data indicate that dinucleotide cap analogs containing guanine base in the first transcribed nucleotide are more susceptible to enzymatic digestion by hNudt16 than their counterparts containing adenine. m^7GpppG, m^7Gpppm$^{2'\text{-}O}$G, and $m_3^{2,2,7}$GpppG were hydrolyzed by hNudt16 with a comparable rate. After 100 min of incubation with hNudt16 (0.9 μM in reaction mixture), approximately 75% of m^7GpppG and m^7Gpppm$^{2'\text{-}O}$G were converted to m^7GDP and GMP/m$^{2'\text{-}O}$GMP, respectively. m^7GpppA and m^7Gpppm$^{2'\text{-}O}$A seemed less susceptible to enzymatic cleavage. A small proportion of those compounds were hydrolyzed simultaneously during incubation with the enzyme. Unmethylated dinucleotides, GpppG and ApppG, were also hydrolyzed by hNudt16, albeit

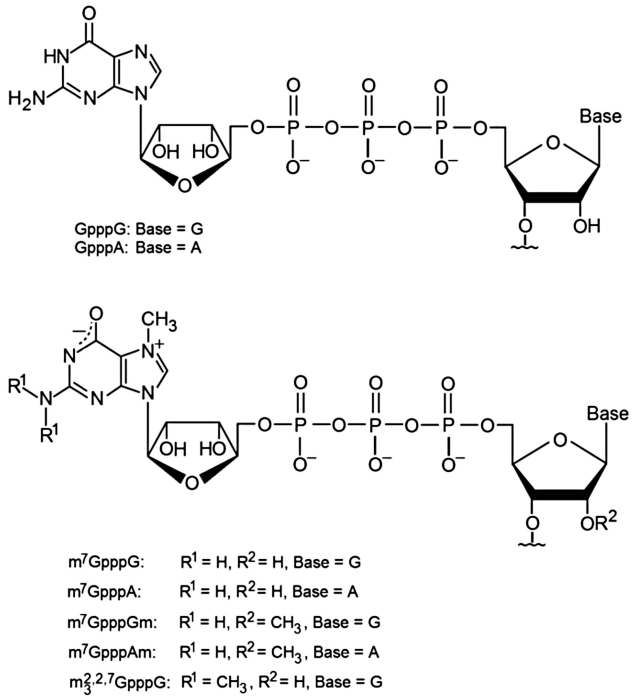

Figure 1. Structures of the dinucleotides used in the present study.

with greater efficiency than for m^7GpppG and m^7Gpppm$^{2'\text{-}O}$G. However, no hydrolysis products were detected for m^7Gpppm^{7}G.

Hydrolytic susceptibility of capped oligonucleotides to hNudt16-mediated hydrolysis

Further, we analyzed the hydrolytic susceptibility of short oligonucleotides capped with the same aforementioned dinucleotides. These oligonucleotides were transcribed in vitro and incubated with recombinant hNudt16 to initiate the decapping process. At different time points (5, 15, 30, 60, and 180 min, and 24 h), enzymatic reactions were terminated and the reaction mixtures were analyzed on a sequencing gel, stained with a fluorescent dye, and visualized using a UV-transilluminator. Levels of decapped transcripts were determined through densitometric analysis. The results of decapping of GpppG-16nt and m^7GpppG-16nt are presented in Figure 3A–C. In both cases, the capped oligonucleotides (marked with C) migrate slower than the decapped products (marked with D). Bands migrating above the capped bands resulted from the inherent ability of T7 polymerase to transcribe certain oligonucleotides containing one or more additional nontemplate nucleotides at the 3′ end (Milligan et al. 1987). There was also a small amount of decapped product at time 0, increasing from incomplete capping during in vitro transcription which hardly ever is 100% efficient. During the first 15 min of the reaction, GpppG-16nt was hydrolyzed twofold more efficiently than m^7GpppG-16nt; however, after a longer duration (1 h), the extent of decapped products was similar for both transcripts. The same effect was observed for $m_3^{2,2,7}$GpppG-16nt (Fig. 3B,C).

The results of hydrolysis of all investigated oligonucleotides are summarized in Table 2. Our data indicate similar decapping efficiency for transcripts with m^7GpppG, m^7Gpppm$^{2'\text{-}O}$G, and $m_3^{2,2,7}$GpppG. Approximately 80% of the three compounds was hydrolyzed during 60 min. Transcripts containing m^7GpppA and m^7Gpppm$^{2'\text{-}O}$A underwent cap cleavage at a significantly lower rate. During 60 min of the reaction, only 5% of both substrates were hydrolyzed and 50% of decapping was achieved after a prolonged duration (24 h) of incubation. Interestingly, GpppG-16nt and GpppA-16nt oligonucleotides proved to be more susceptible to enzymatic cleavage by hNudt16 than their methylated counterparts. A significant difference was observed at the initial stage of hydrolysis (15 min); however, after a longer duration (60 min), the extent of decapping was comparable for all transcripts.

Analysis of the hydrolysis of longer transcripts (GpppG-34nt, m^7GpppG-34nt, m^7Gpppm$^{2'\text{-}O}$G-34nt) (Fig. 3D) indicates the same tendency, as observed for dinucleotides and short oligonucleotides (16 nt). As shown in Table 2, decapping efficiency determined at different time points of the reaction is nearly equal for transcripts m^7GpppG-34nt and m^7Gpppm$^{2'\text{-}O}$G-34nt, but significantly higher for GpppG-34nt. During the first 5 min of hydrolysis, approximately 50% of unmethylated transcript GpppG-34nt was hydrolyzed. Simultaneously, only a small proportion of methylated oligonucleotides was decapped, although the enzyme levels in the reaction mixture were fivefold higher. Hydrolysis was more efficient for transcripts containing 16 nt than for their counterparts containing 34 nt.

The results obtained for oligonucleotides are concurrent with those for dinucleotides, indicating the crucial role of guanine base in the first transcribed nucleotide for efficient decapping by hNudt16. However, the difference in decapping efficiency between methylated and unmethylated species was most significant for transcripts containing 34 nt.

Hydrolysis of capped oligonucleotides catalyzed by the Dcp1/Dcp2 complex

Selected oligonucleotides (m^7GpppG-16nt, m^7GpppG-34nt, and m^7Gpppm$^{2'\text{-}O}$G-34nt) were hydrolyzed by the *Schizosaccharomyces pombe* Dcp1/Dcp2 complex. Electrophoresis and evaluation of hydrolysis efficiency obtained through densitometric analysis are shown in Figure 3. Our data indicate that m^7GpppG-34nt and m^7Gpppm$^{2'\text{-}O}$G-34nt rather than m^7GpppG-16nt were hydrolyzed more efficiently by Dcp1/Dcp2. According to the current literature, Dcp2 can hydrolyze capped transcripts that are at least 26 nt long (Scarsdale et al. 2006). Our results are concurrent with the published data. In our experiments, longer transcripts (GpppG-34nt, m^7GpppG-34nt, and

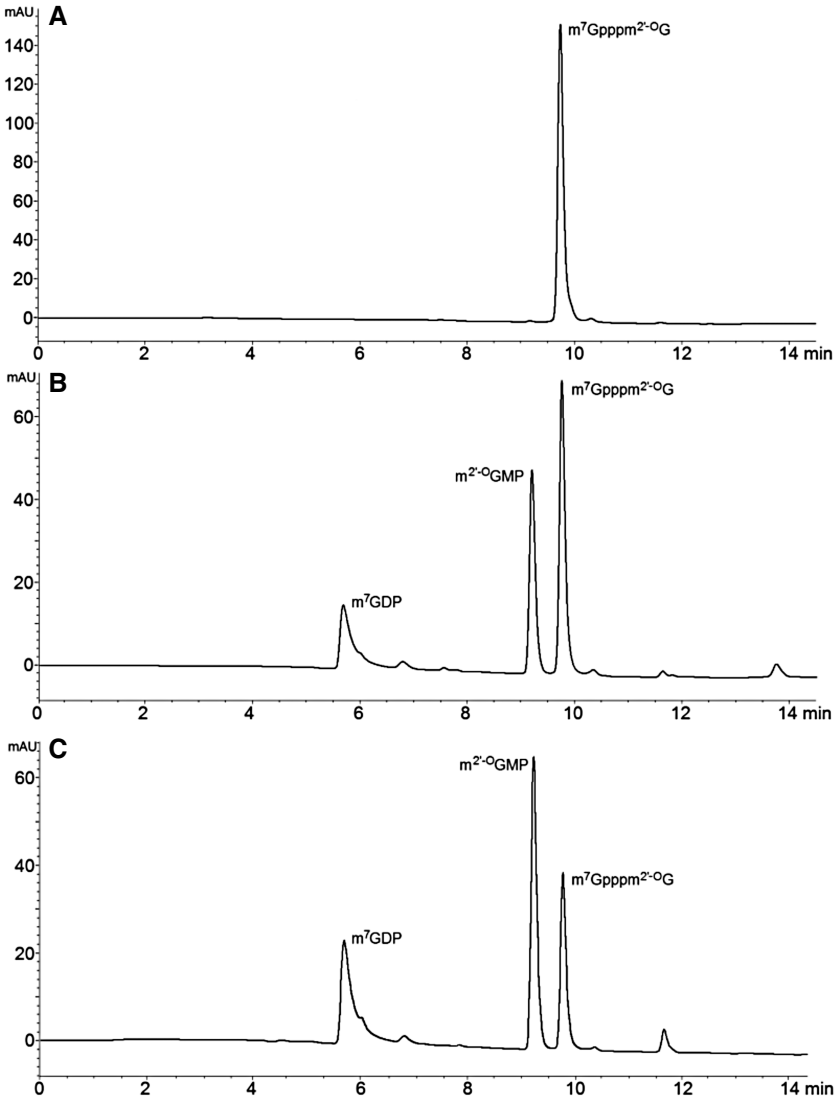

Figure 2. HPLC profiles of $m^7Gpppm^{2'-O}G$ hydrolyzed with recombinant hNudt16: (*A*) before hydrolysis, (*B*) after 60 min of hydrolysis, (*C*) after 100 min of hydrolysis. Reaction was performed at 37°C, in 40 mM Tris buffer (pH 7.9) containing 100 mM NaCl, 6 mM $MgCl_2$, and 2 mM DTT.

$m^7Gpppm^{2'-O}G$-34nt) were mostly hydrolyzed during 5 min of incubation with the enzyme, whereas the shorter one (m^7GpppG-16nt) was hydrolyzed only to a small extent after 60 min of incubation with the enzyme. Dcp1/Dcp2 levels in the reaction mixture were 50 nM, approximately 400 times lower than those of hNudt16 (18 μM) in reactions with the same substrates. This comparison indicates much higher catalytic efficiency of the Dcp1/Dcp2 complex toward capped oligonucleotides than of hNudt16.

DISCUSSION

The Nudix family of hydrolases comprises numerous enzymes with various functions. Many of them catabolize various substrates including canonical (d)NTPs, oxidized (d)NTPs, non-nucleoside polyphosphates, and capped mRNAs (Mildvan et al. 2005). The present study focused on hNudt16 and its hydrolytic activity toward dinucleotide cap analogs and short capped oligonucleotides. Previously, it was reported that this enzyme has mRNA decapping activity; however, the diversity of naturally occurring cap structures was not addressed. Hence, we investigated several dinucleotide cap analogs as potential substrates of this enzyme. Our results confirmed the previously reported data that hNudt16 hydrolyzes the dinucleotide cap analog m^7GpppG, yielding m^7GDP and GMP (Song et al. 2010). Moreover, we report that the other cap analogs containing additional methylations and bearing guanine base in the first transcribed nucleotide ($m^7Gpppm^{2'-O}G$ and $m_3^{2,2,7}GpppG$) were also hydrolyzed by hNudt16, with an efficiency comparable to that for m^7GpppG hydrolysis. In contrast, cap analogs with adenine (m^7GpppA and $m^7Gpppm^{2'-O}A$) were significantly less susceptible to enzymatic cleavage. These data were unexpected, as the previously reported crystal structure of *Xenopus laevis* Nudt16 with m^7GpppA dinucleotide displayed binding via the adenine part of the cap, while m^7G protruded outward with little or no interaction with the protein (Fig. 4; Scarsdale et al. 2006). Notably, depending on the identity of the base, nucleosides adopt an *anti* or *syn* conformation for guanosine and adenosine, respectively, upon binding, probably because the protein's capacity to bind the adenine-containing compounds was preserved in the conformation that prevents hydrolysis.

Our results show that dinucleotides methylated at the N(7) position of guanine are worse substrates for hNudt16. Moreover, in the case of m^7GpppG and GpppG, we observed the release of m^7GDP and GDP, respectively; however, only GDP was rapidly converted to GMP. We also assessed the two-headed m^7Gpppm^7G dinucleotide, which proved to be resistant to hydrolysis, thereby indicating that Nudt16 cannot hydrolyze N(7)-methylated substrates. Investigation of the crystal structure of GTP-bound Nudt16 suggests the possibility of there being enough space to accommodate m^7G, as N(7) has no direct interaction with the protein side chains, but the positive charge at the methylated N(7) position may negatively impact binding, thereby inhibiting hydrolysis.

Table 1. Hydrolysis of dinucleotide cap analogs catalyzed by recombinant hNudt16

	% of hydrolyzed dinucleotide after indicated time of reaction						
Dinucleotide	10 min	20 min	30 min	40 min	60 min	80 min	100 min
GpppG	42.67 ± 3.28	66.47 ± 2.89	83.35 ± 4.04	98.79 ± 6.11	–	–	–
ApppG	24.67 ± 3.34	43.11 ± 4.82	55.04 ± 8.02	62.94 ± 3.66	75.71 ± 5.85	86.87 ± 7.44	94.32 ± 11.22
m^7GpppG	17.63 ± 1.28	29.44 ± 3.73	39.67 ± 5.34	45.18 ± 4.98	54.36 ± 7.12	67.43 ± 8.15	72.97 ± 9.48
m^7Gpppm$^{2'\text{-}O}$G	17.55 ± 3.05	29.77 ± 6.24	37.08 ± 4.99	43.98 ± 8.21	56.77 ± 5.72	69.24 ± 7.99	76.89 ± 8.77
$m_3^{2,2,7}$GpppG	10.74 ± 1.89	20.71 ± 3.05	27.18 ± 5.89	33.73 ± 7.39	46.64 ± 9.56	57.23 ± 10.56	64.96 ± 11.27
m^7GpppA	nd	nd	nd	nd	nd	nd	2.57 ± 0.45
m^7Gpppm$^{2'\text{-}O}$A	nd	nd	nd	nd	nd	nd	1.68 ± 0.32
m^7Gpppm^{7}G	nd	nd	nd	nd	nd	nd	nd

Reactions were performed at 37°C, in 40 mM Tris buffer (pH 7.9) containing 100 mM NaCl, 6 mM $MgCl_2$, and 2 mM DTT. Dinucleotide concentration was 15 μM, enzyme concentration 0.9 μM. The extent of decapping was determined as the percentage of hydrolyzed dinucleotide measured by HPLC method (based on the three independent experiments for each compound). (nd, not detected.)

Interestingly, both unmethylated cap analogs, GpppG and ApppG, were hydrolyzed more efficiently than canonical m^7GpppG cap. Since the unmethylated dinucleotide cap structure is symmetrical, it can be accessed from either side by Nudt16. In the case of ApppG, we observed a slight delay in hydrolysis, which can probably be explained by the exclusive cap dinucleotide hydrolysis from the guanosine end.

We also found that hNudt16 can recognize short capped oligonucleotides (16 nt and 34 nt) as substrates. In the case of 16-nt oligonucleotides, we observed an even stronger preference for unmethylated cap structures. Similarly to dinucleotides, additional methyl groups in m^7Gpppm$^{2'\text{-}O}$G- and $m_3^{2,2,7}$GpppG-capped oligonucleotides did not affect rate of the hydrolysis. Furthermore, oligonucleotides containing adenine in the first nucleotide were also processed significantly slower than corresponding substrates with guanine. Considering structures of oligonucleotides, we expected only the external (m^7)Gppp region of the cap to be accessible by Nudt16. Nevertheless, we are unsure whether hydrolysis can occur via binding of the proximal (m^7Gpp), distal (ppG/ppA), or either region of the cap. The observation that unmethylated cap structures in GpppG-16nt and GpppA-16nt are hydrolyzed at a similar rate contrasts that of their m^7G counterparts, wherein one can see a clear preference for m^7GpppG-16nt over m^7GpppA-16nt. We also observed an additional product of GpppG-16nt and GpppA-16nt hydrolysis, which migrated between the capped and uncapped RNA species (Fig. 3), which could have resulted from alternative cap cleavage resulting in a mixture of pG-16nt and ppG-16nt (and their adenine counterparts). However, no such products were observed in the case of methylated m^7GpppG-16nt and m^7GpppA-16nt oligonucleotides, which in turn suggests that methylation at the N(7) position prevents m^7G binding, and the enzyme recognizes only the first transcribed nucleotide. Consequently, hydrolysis of oligonucleotides leads to the generation of exclusively m^7GDP and pA-16nt/pG-16nt.

A significant effect of adenosine on hydrolysis was unexpected, considering that Nudt16 was initially found to cleave the hypermethylated cap bound to adenosine ($m_3^{2,2,7}$GpppA) present at the 5′ end of U8 snoRNA (Lange et al. 1998). It is, however, notable that Nudt16 binds U8 snoRNA regardless of the presence of the cap structure, thus indicating the possible importance of RNA secondary structures that can interact with the cationic surface of the protein.

Hydrolytic activity toward the dinucleotide cap structures in cells is attributed to the scavenger decapping enzyme (DcpS), which is involved in the last step of the 3′→5′ mRNA degradation pathway. hNudt16 can also hydrolyze dinucleotide cap analogs; however, its activity toward m^7GpppG is significantly lower than that observed for hDcpS (Song et al. 2010). Substrate specificity of hNudt16 is also different from that of hDcpS. The preferred substrate for hDcpS is m^7GpppG, while GpppG is hydrolyzed less efficiently and $m_3^{2,2,7}$GpppG is resistant to hydrolysis by this enzyme. In contrast, hNudt16 hydrolyzes m^7GpppG and $m_3^{2,2,7}$GpppG with comparable rates; however, it hydrolyzes unmethylated dinucleotides, GpppG and ApppG, more efficiently. We also compared decapping activities of hNudt16 toward m^7GpppG-34nt and m^7Gpppm$^{2'\text{-}O}$G-34nt with that of Dcp2. For both transcripts, decapping efficiency was significantly higher in the presence of Dcp2. Nonetheless, none of these enzymes can hydrolyze oligonucleotides longer than 10 nt and shorter than 25 nt. However, it is unclear whether hNudt16 has an additional role in the mRNA decapping process. If such a role is biologically significant, hNudt16 activity would be enhanced by an unknown partner protein. However, it is more probable that hNudt16 is engaged in cellular functions other than RNA decapping. Moreover, hNudt6 was reported to hydrolyze several other purine nucleoside diphosphates and cleave pyrophosphate

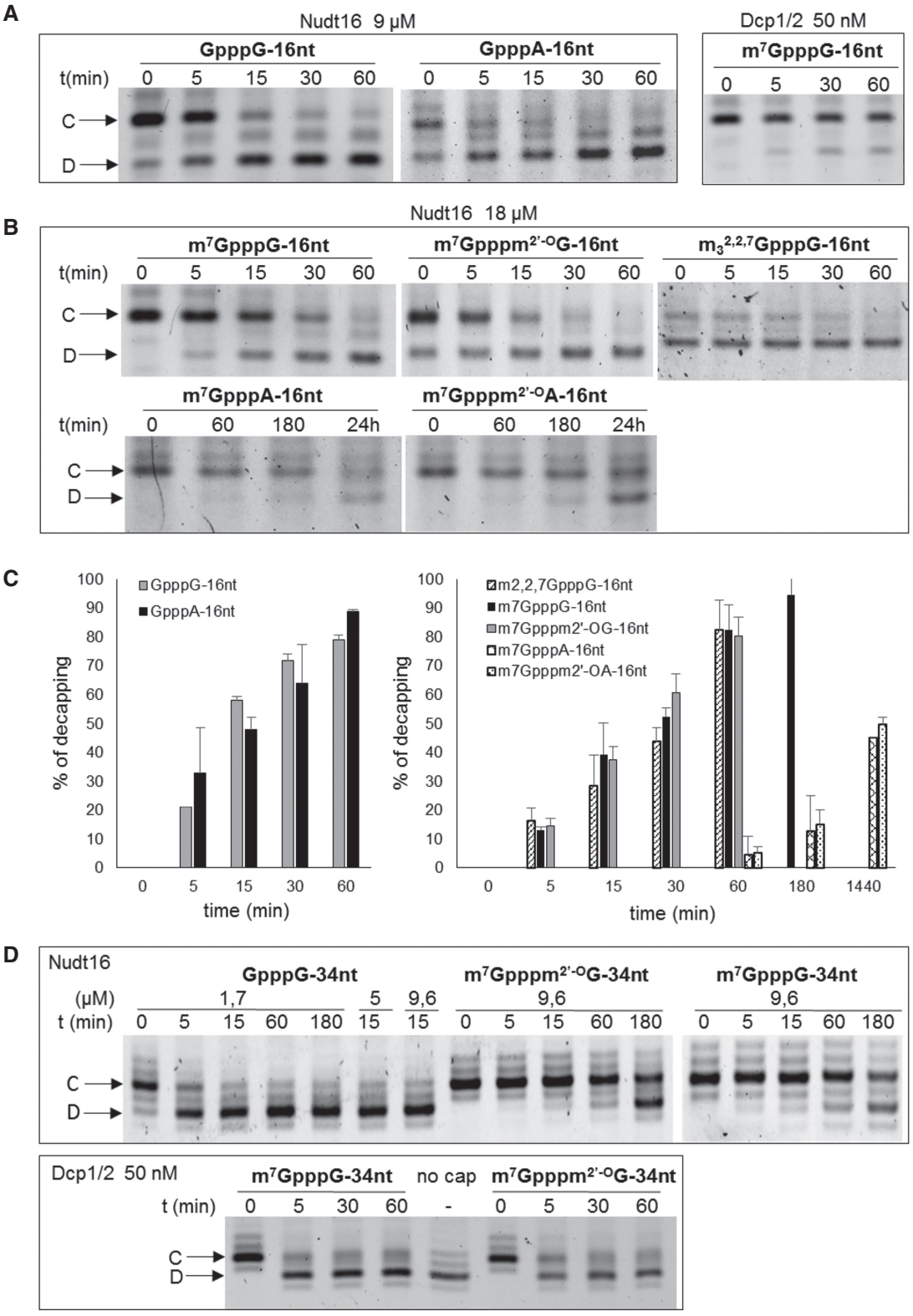

Figure 3. Hydrolysis of capped oligonucleotides by hNudt16. (*A*) Gel electrophoretic analysis of the progress of the hydrolysis of GpppG-16nt and GpppA-16nt. For comparison, reaction with Dcp1/2 was performed for m^7GpppG-16nt. (*B*) Gel electrophoretic analysis of 16-nt oligonucleotides bearing different cap structures. (*C*) Comparison of decapping yield for capped and uncapped 16-nt oligonucleotides. (*D*) Gel electrophoretic analysis of decapping for methylated and unmethylated 34-nt oligonucleotides. All oligonucleotides were treated with recombinant hNudt16 at 30°C in 50 mM Tris buffer (pH 7.9) containing 10 mM NaCl, 6 mM $MgCl_2$, 10 mM DTT, and 1 mM spermidine. The decapping percentage was calculated as the percent loss in the capped band, normalized by total quantity in the capped and decapped bands.

Table 2. Hydrolysis of differently capped 16-nt RNAs by recombinant hNudt16

Cap analog at 5′ end of 16-nt mRNA	Nudt16	RNA:Nudt16	% of decapping after indicated time					
			5 min	15 min	30 min	60 min	180 min	24 h
GpppG (1 μM)	0.9 μM	1:0.9	21.45 ± 0.08	58.86 ± 1.45	72.14 ± 2.04	79.87 ± 1.71	–	–
GpppG (1 μM)	18 μM	1:18	–	85.80	–	85.48	86.90	–
m^7GpppG (1 μM)	18 μM	1:18	13.09 ± 1.16	39.40 ± 10.84	52.55 ± 2.85	82.63 ± 8.67	94.76 ± 6.78	–
$m^7Gpppm^{2'\text{-}O}G$ (1 μM)	18 μM	1:18	14.50 ± 2.65	37.34 ± 4.72	60.89 ± 6.30	80.52 ± 6.57	–	–
GpppA (1 μM)	0.9 μM	1:0.9	32.99 ± 15.75	48.45 ± 4.30	63.88 ± 13.43	89.75 ± 0.47	–	–
m^7GpppA (1 μM)	18 μM	1:18	–	–	–	4.62 ± 6.44	12.75 ± 12.15	45.19 ± 0.01
$m^7Gpppm^{2'\text{-}O}A$ (1 μM)	18 μM	1:18	–	–	–	5.21 ± 2.29	15.07 ± 5.07	49.65 ± 2.63
TMG (1 μM)	18 μM	1:18	16.47 ± 4.47	28.54 ± 10.70	43.80 ± 4.86	82.62 ± 10.35	–	–

Cap analog at 5′ end of 34-nt mRNA	Nudt16	RNA:Nudt16	% of decapping after indicated time			
			5 min	15 min	60 min	180 min
GpppG (0.23 μM)	1.7 μM	1:7.4	46.8 ± 10.84	70 ± 5.66	80.69 ± 2.51	81.44 ± 2.39
GpppG (0.23 μM)	9.6 μM	1:42	–	75.30 ± 3.35	–	–
m^7GpppG (0.23 μM)	9.6 μM	1:42	3.2 ± 1.58	8.77 ± 1.84	26.25 ± 5.15	51.85 ± 4.32
$m^7Gpppm^{2'\text{-}O}G$ (0.23 μM)	9.6 μM	1:42	1.04 ± 1.81	8.23 ± 2.02	27.14 ± 6.47	43.86 ± 15.00

The capped RNAs were prepared by in vitro transcription and incubated with hNudt16 during indicated time periods. The reaction mixtures were analyzed on a sequencing gel and stained with fluorescent dye. The decapping percentage was calculated as the percentage loss in the capped band, normalized by total quantity in the capped and decapped bands.

groups in ADP-ribosylated proteins. Considering the structural similarities, the ability of hNudt16 to hydrolyze the cap structure could result from its inability to completely distinguish between various purine diphosphate substructures.

MATERIALS AND METHODS

Chemical synthesis of cap analogs

Cap analogs (m^7GpppG, $m^7Gpppm^{2'\text{-}O}G$, $m_3^{2,2,7}$GpppG, m^7GpppA, and $m^7Gpppm^{2'\text{-}O}A$) and unmethylated dinucleotides (ApppG and GpppG) were synthesized in accordance with the previously described procedures (Darzynkiewicz et al. 1990; Stepinski et al. 1995; Jankowska et al. 1996; Niedzwiecka et al. 2007).

In vitro synthesis of short oligonucleotides and capping reaction

DNA templates for the generation of short RNAs of 16 and 34 nt were prepared through XhoI or EcoRI cleavage of pSPluc+ plasmid containing either the T7 class III promoter (ϕ6.5) or the class II promoter (ϕ2.5). ppp-RNAs were transcribed in vitro with the T7 RNA polymerase in the presence of four nucleotides, as described by Strenkowska et al. (2016). TMG and TMA capped transcripts were obtained by replacing GTP or ATP with 5:1 $m_3^{2,2,7}$GpppG:GTP or $m_3^{2,2,7}$GpppA:ATP, respectively. m^7Gppp-RNA and Gppp-RNA were prepared through posttranscriptional capping of ppp-RNA with the ScriptCap m^7G Capping System (CellScript) with or without *S*-adenosylmethionine (SAM) in accordance with the manufacturer's instructions. Briefly, 10 μg samples of RNA were heat-denaturated at 65°C for 5 min, cooled on ice, and incubated with ScriptCap Buffer in the presence of 1 mM GTP, 100 μM SAM, 10 U Vaccinia Capping Enzyme, and Script Guard RNase Inhibitor for 3 h at 37°C. Cap1-RNA was obtained through simultaneous capping and 2′-*O*-Methylation from uncapped RNA, using ScriptCap m^7G Capping System and the ScriptCap 2′-*O*-Methyltransferase Kit. RNAs were purified using the Oligo Clean-up and Concentration Kit (Norgen Biotek) and analyzed through denaturing PAGE on a 15% polyacrylamide/7 M urea containing gel. Small amounts of $n+1$ and $n+2$ contaminations originated from the nontemplated addition of nucleotides during in vitro transcription.

Protein expression and purification

Human Nudt16 (hNudt16, 1–199 aa, MW 22 kDa) was expressed in *E. coli* Rosetta 2 (DE3) as a C-terminally His-tagged protein using a peET16b_Nudt16 vector, where the coding sequence of Nudt16 was cloned at the NcoI–BamHI restriction sites (verified further through sequencing). A sequence encoding four additional histidine residues introduced immediately after the two terminal histidine residues of Nudt16 resulted in the formation of a 6× His C-terminal His-tag. The complete protocol of hNudt16 preparation and purification has been presented previously by Wojtczak et al. (2016). Fractions of pure enzyme were dialyzed against 50 mM Tris-HCl pH 8.0, 150 mM KCl, and 20% glycerol. Aliquots of hNudt16 were supplemented with 1 mM DTT, frozen in liquid nitrogen, and stored at −80°C until use.

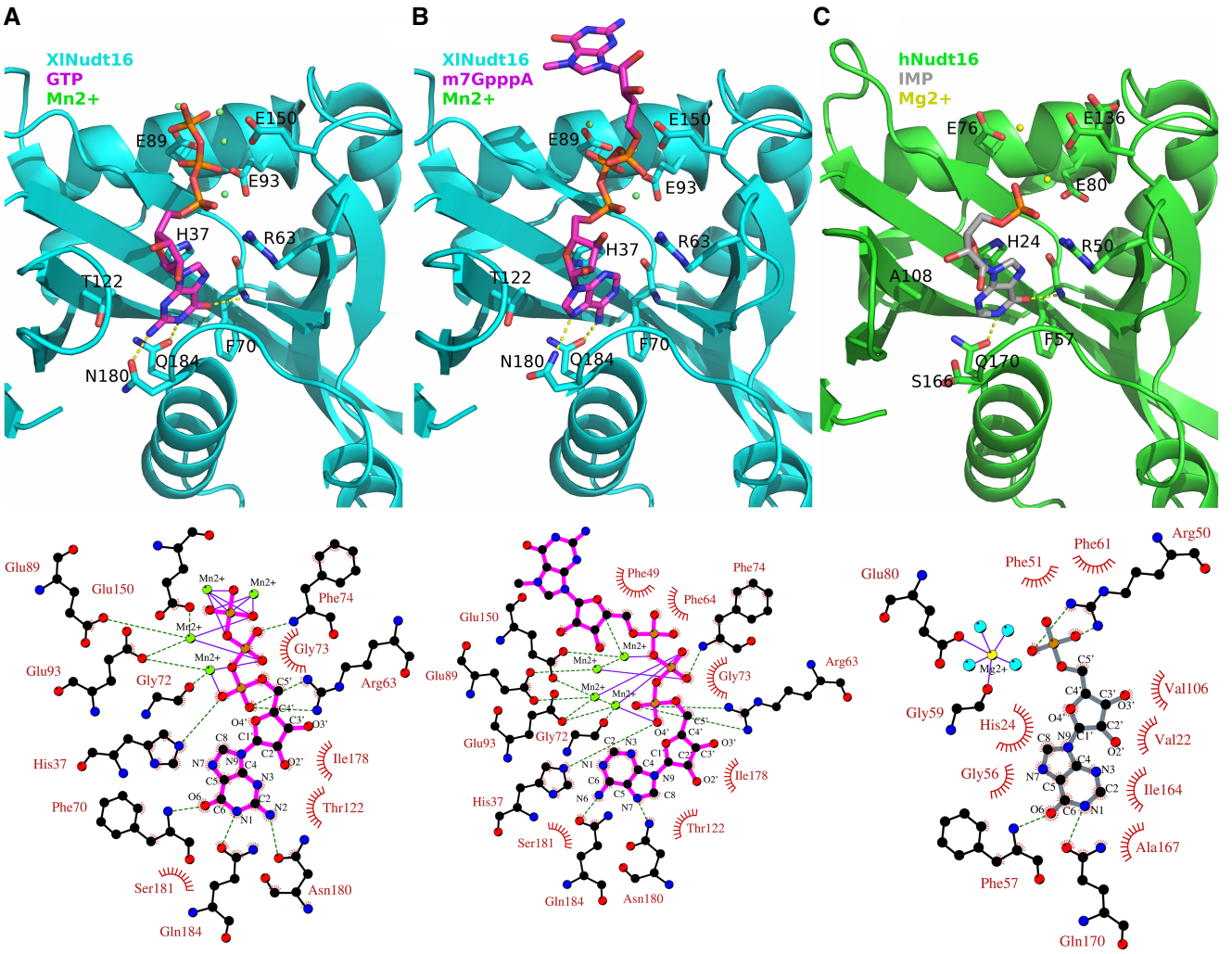

Figure 4. Interactions between Nudt16 and its ligands. (*A*) (*Upper* panel) Visualization of the GTP-bound XL Nudt16 active site (PDB 2A8S). Color codes for the protein, ligand, and metal ions are indicated. For clarity, only interactions with the base and selected residues are shown. (*Lower* panel) Ligplot (Wallace et al. 1995) representation of the structure shown in the *upper* panel. (*B*) (*Upper* panel) Visualization of the XL Nudt16 active site with m^7GpppA. Color codes are the same as those in *A*. (*C*) (*Upper* panel) Visualization of the IMP-bound hNudt16 active site (PDB: 2XSQ). (*Lower* panel) Ligplot representation of the structure shown in the *upper* panel.

Decapping assays

Enzymatic assays for dinucleotides were performed in 40 mM Tris buffer (pH 7.9) containing 100 mM NaCl, 6 mM $MgCl_2$ and 2 mM DTT. The concentration of investigated dinucleotides was 15 µM, and enzyme concentration was 0.9 µM for each substrate. Decapping assays for short oligonucleotides were performed in 50 mM Tris buffer (pH 7.9) containing 10 mM NaCl, 6 mM $MgCl_2$, 10 mM DTT, and 1 mM spermidine.

Determination of hydrolytic susceptibility of cap analogs

To investigate the hydrolytic susceptibility of dinucleotide cap analogs, HPLC analysis was performed. Before each experiment, 1 mL of buffer solution containing the analyte was incubated at 37°C for 10 min. Hydrolysis was initiated through the addition of recombinant hNudt16. After 10, 20, 30, 40, and 60 min of hydrolysis, 150-µL aliquots of the reaction mixture were withdrawn and incubated at 97°C during 3 min to terminate the reaction through heat inactivation of the enzyme. The samples were then subjected to HPLC analysis (Agilent 1200 Series) with a reverse-phase Supelcosil LC-18-T column and UV/VIS-detector. The substrate and products were eluted at 20°C with a linear gradient of methanol in 0.1 M KH_2PO_4 (from 0% to 40%) over 15 min at a flow rate of 1.0 mL/min. Changes in absorbance values at 260 nm were monitored continuously during the analysis. Hydrolysis products were identified through comparison of their retention times with that of the reference samples. The extent of decapping, determined as the percentage of hydrolyzed substrate, was calculated using area under the chromatographic peak of respective compounds.

To assess the decapping of short oligonucleotides, 20 ng of capped transcripts were digested with different amounts of hNudt16, at

30°C. Reactions were terminated at different time points (15 min, 30 min, 1 h, and 3 h) by cooling the reaction mixture on ice and adding FORMAzol, followed by denaturation for 3 min at 55°C. The substrates and products were separated on an RNA sequencing gel (15% polyacrylamide, 7 M urea) stained with a fluorescent dye (SYBR Gold Nucleic Acid Gel Stain, Life Technologies) and visualized using a UV-transilluminator (ChemiDoc MP Imaging System, Bio-Rad). The amount of capped substrates and decapped products were determined through densitometric analysis, and the decapping percentage was calculated as the percent loss in the capped band, normalized by total quantity in the capped and decapped bands. Quantity of material in individual bands was analyzed using Image Lab Software (Bio-Rad).

ACKNOWLEDGMENTS

We thank M. Kiledjian for helpful discussions and critical reading of the manuscript and J. Zuberek and A. Stelmachowska for SpDcp1/2 protein preparation. This study was supported by grants from the Polish National Science Centre (UMO/2013/08/A/NZ1/00866 and DEC-2013/11B/ST5/02226) and the National Centre of Research and Development (STRATEGMED1/235773/19/NCBR/2016).

Received January 15, 2018; accepted February 20, 2018.

REFERENCES

Arribas-Layton M, Wu D, Lykke-Andersen J, Song H. 2013. Structural and functional control of the eukaryotic mRNA decapping machinery. *Biochim Biophys Acta* **1829:** 580–589.

Bessman MJ, Frick DN, O'Handley SF. 1996. The MutT proteins or "Nudix" hydrolases, a family of versatile, widely distributed, "housecleaning" enzymes. *J Biol Chem* **271:** 25059–25062.

Carreras-Puigvert J, Zitnik M, Jemth AS, Carter M, Unterlass JE, Hallström B, Loseva O, Karem Z, Calderón-Montaño JM, Lindskog C, et al. 2017. A comprehensive structural, biochemical and biological profiling of the human NUDIX hydrolase family. *Nat Commun* **8:** 1541.

Cohen LS, Mikhli C, Jiao X, Kiledjian M, Kunkel G. 2005. Dcp2 decaps $m_3^{2,2,7}$GpppN capped RNAs, and its activity is sequence and context dependent. *Mol Cell Biol* **25:** 8779–8791.

Daniels D, Thirawatananond P, Ong SE, Grabelli SB, Leung AKL. 2015. Nudix hydrolases degrade protein-conjugated ADP-ribose. *Sci Rep* **5:** 18271.

Darzynkiewicz E, Stepinski J, Tahara SM, Stolarski R, Ekiel I, Haber D, Neuvonen K, Lehikoinen P, Labádi I, Lönnberg H. 1990. Synthesis, conformation and hydrolytic stability of P^1,P^3-dinucleoside triphosphates related to mRNA 5′-cap, and comparative kinetic studies on their nucleoside and nucleoside monophosphate analogues. *Nucleosides Nucleotides* **9:** 599–618.

Deshmukh MV, Jones BN, Quang-Dang DU, Flinders J, Floor SN. 2008. mRNA decapping is promoted by an RNA-binding channel in Dcp2. *Mol Cell* **29:** 324–336.

Franks TM, Lykke-Andersen J. 2008. The control of mRNA decapping and P-body formation. *Mol Cell* **32:** 605–615.

Furuichi Y, Shatkin AJ. 2000. Viral and cellular mRNA capping: past and prospects. *Adv Virus Res* **55:** 135–184.

Ghosh A, Lima CD. 2010. Enzymology of RNA cap synthesis. *Wiley Interdiscip Rev RNA* **1:** 152–172.

Ghosh T, Peterson B, Tomasevic N, Peculis BA. 2004. *Xenopus* U8 snoRNA binding protein is a conserved nuclear decapping enzyme. *Mol Cell* **13:** 817–828.

Grudzien-Nogalska E, Kiledjian M. 2017. New insights into decapping enzymes and selective mRNA decay. *Wiley Interdiscip Rev RNA* **8.** doi: 10.1002/wrna.1379.

Iwasaki S, Takeda A, Motose H, Watanabe Y. 2007. Characterization of *Arabidopsis* decapping proteins AtDCP1 and AtDCP2, which are essential for post-embryonic development. *FEBS Lett* **581:** 2455–2459.

Iyama T, Abolhassani N, Tsuchimoto D, Nonaka M, Nakabeppu Y. 2010. NUDT16 is a (deoxy)inosine diphosphatase, and its deficiency induces accumulation of single-strand breaks in nuclear DNA and growth arrest. *Nucleic Acids Res* **38:** 4834–4843.

Jankowska M, Stępiński J, Stolarski R, Wieczorek Z, Temeriusz A, Haber D, Darżynkiewicz E. 1996. ^{1}H NMR and fluorescence studies of new mRNA 5′-cap analogues. *Collect Czech Chem Commun* **61:** S197–S202.

Lange TS, Borovjagin AV, Gerbi SA. 1998. Nucleolar localization elements in U8 snoRNA differ from sequences required for rRNA processing. *RNA* **4:** 789–800.

Li Y, Song MG, Kiledjian M. 2008. Transcript-specific decapping and regulated stability by the human Dcp2 decapping protein. *Mol Cell Biol* **28:** 939–948.

Li Y, Song M, Kiledjian M. 2011. Differential utilization of decapping enzymes in mammalian mRNA decay pathways. *RNA* **17:** 419–428.

Liu H, Rodgers ND, Jiao X, Kiledjian M. 2002. The scavenger mRNA decapping enzyme DcpS is a member of the HIT family of pyrophosphatases. *EMBO J* **21:** 4699–4708.

Liu SW, Jiao X, Liu H, Gu M, Lima CD, Kiledjian M. 2004. Functional analysis of mRNA scavenger decapping enzymes. *RNA* **10:** 1412–1422.

Lu G, Zhang J, Li Y, Li Z, Zhang N, Xu X, Wang T, Guan Z, Gao G, Yan J. 2011. hNudt16: a universal decapping enzyme for small nucleolar RNA and cytoplasmic mRNA. *Protein Cell* **2:** 64–73.

McLennan AG. 2006. The Nudix hydrolase superfamily. *Cell Mol Life Sci* **63:** 123–143.

Meyer S, Temme C, Wahle E. 2004. Messenger RNA turnover in eukaryotes: pathways and enzymes. *Crit Rev Biochem Mol Biol* **39:** 197–216.

Mildvan AS, Xia Z, Azurmendi HF, Saraswat V, Legler PM, Massiah MA, Gabelli SB, Bianchet MA, Kang LW, Amzel LM. 2005. Structures and mechanisms of Nudix hydrolases. *Arch Biochem Biophys* **433:** 129–143.

Milligan JF, Groebe DR, Witherell GW, Uhlenbeck OC. 1987. Oligoribonucleotide synthesis using T7 RNA polymerase and synthetic DNA templates. *Nucleic Acids Res* **15:** 8783–8798.

Niedzwiecka A, Stepinski J, Antosiewicz JM, Darzynkiewicz E, Stolarski R. 2007. Biophysical approach to studies of cap-eIF4E interaction by synthetic cap analogs. *Methods Enzymol* **430:** 209–245.

Palazzo L, Thomas B, Jemth AS, Colby T, Leidecker O, Feijs KL, Zaja R, Loseva O, Puigvert JC, Matic I, et al. 2015. Processing of protein ADP-ribosylation by Nudix hydrolases. *Biochem J* **468:** 293–301.

Peculis BA, Reynolds K, Cleland M. 2007. Metal determines efficiency and substrate specificity of the nuclear NUDIX decapping proteins X29 and H29K (Nudt16). *J Biol Chem* **282:** 24792–24805.

Picirillo C, Khanna R, Kiledjian M. 2003. Functional characterization of the mammalian mRNA decapping enzyme hDcp2. *RNA* **9:** 1138–1147.

Scarsdale JN, Peculis BA, Wright HW. 2006. Crystal structures of U8 snoRNA decapping nudix hydrolase, X29, and its metal and cap complex. *Structure* **14:** 331–343.

Schaeffer D, Tsanova B, Barbas A, Reis FP, Dastidar EG, Sanchez-Rotunno M, Arraiano CM, van Hoof A. 2009. The exosome contains domains with specific endoribonuclease, exoribonuclease and cytoplasmic mRNA decay activities. *Nat Struct Mol Biol* **16:** 56–62.

Song M, Li Y, Kiledjian M. 2010. Multiple mRNA decapping enzymes in mammalian cells. *Mol Cell* **40:** 423–432.

Steiger M, Carr-Schmidt A, Schwartz DC, Kiledjian M, Parker R. 2003. Analysis of recombinant yeast decapping enzyme. *RNA* **9:** 231–238.

Stepinski J, Bretner M, Jankowska M, Felczak K, Stolarski R, Wieczorek Z, Caipostalcode AL, Rhoads RE, Temeriusz A, Haber D, et al. 1995. Synthesis and properties of P^1, P^2-, P^1, P^3, and P^1, P^4-dinucleoside di-, tri- and tetraphosphate mRNA 5′-cap analogues. *Nucleosides Nucleotides* **14:** 717–721.

Strenkowska M, Grzela R, Majewski M, Wnek K, Kowalska J, Lukaszewicz M, Zuberek J, Darzynkiewicz E, Kuhn AN, Sahin U, Jemielity J. 2016. Cap analogs modified with 1,2-dithiodiphosphate moiety protect mRNA from decapping and enhance its translational potential. *Nucleic Acids Res* **44:** 9578–9590.

Taylor MJ, Peculis B. 2008. Evolutionary conservation supports ancient origin for Nudt16, a nuclear-localized, RNA-binding, RNA-decapping enzyme. *Nucleic Acids Res* **36:** 6021–6034.

Trésaugues L, Lundbäck T, Welin M, Flodin S, Numan T, Silvander C, Gräslund S, Nordlund P. 2015. Structural basis for the specificity of human NUDT16 and its regulation by inosine monophosphate. *PLoS ONE* **10:** e0131507.

Valkov E, Jonas S, Weichenrieder O. 2017. *Mille viae* in eukaryotic mRNA decapping. *Curr Opin Struct Biol* **47:** 40–51.

van Dijk E, Cougot N, Meyer S, Wahle E. 2002. Human Dcp2: a catalytically active mRNA decapping enzyme located in specific cytoplasmic structures. *EMBO J* **21:** 6915–6924.

Wallace AC, Laskowski RA, Thornton JM. 1995. LIGPLOT: a program to generate schematic diagrams of protein-ligand interactions. *Protein Eng* **8:** 127–134.

Wojtczak BA, Warminski M, Kowalska J, Lukaszewicz M, Honcharenko M, Smith CIE, Strömberg R, Darzynkiewicz E, Jemielity J. 2016. Clickable trimethylguanosine cap analogs modified within the triphosphate bridge: synthesis, conjugation to RNA and susceptibility to degradation. *RSC Advances* **6:** 8317–8328.